VIP Electrochemistry Very Important Paper

Deutsche Ausgabe: DOI: 10.1002/ange.201501005
Internationale Ausgabe: DOI: 10.1002/anie.201501005

Improving the Electrochemical Performance of the $Li_4Ti_5O_{12}$ Electrode in a Rechargeable Magnesium Battery by Lithium–Magnesium Co-Intercalation**

*Na Wu, Zhen-Zhong Yang, Hu-Rong Yao, Ya-Xia Yin, Lin Gu, and Yu-Guo Guo**

Abstract: *Rechargeable magnesium batteries have attracted recent research attention because of abundant raw materials and their relatively low-price and high-safety characteristics. However, the sluggish kinetics of the intercalated Mg^{2+} ions in the electrode materials originates from the high polarizing ability of the Mg^{2+} ion and hinders its electrochemical properties. Here we report a facile approach to improve the electrochemical energy storage capability of the $Li_4Ti_5O_{12}$ electrode in a Mg battery system by the synergy between Mg^{2+} and Li^+ ions. By tuning the hybrid electrolyte of Mg^{2+} and Li^+ ions, both the reversible capacity and the kinetic properties of large $Li_4Ti_5O_{12}$ nanoparticles attain remarkable improvement.*

With growing concern over issues of environmental and sustainable energy supply, researchers have begun to focus on developing clean green-energy storage systems[1] with higher volumetric energy density, lower price, and improved safety. Rechargeable Mg batteries could be a candidate of cost-effective, safe, and environmentally friendly battery systems.[2] However the development of Mg system suffers from several serious limitations, such as metallic Mg/electrolyte incompatibility and the sluggish kinetics of intercalating Mg^{2+} ions in solid electrode hosts originating from the high polarizing ability of Mg^{2+} cations.[3]

Only a few metal/alloy anode and ion insertion-type anode materials[4] exhibiting reasonable discharge capacity and cycling endurance have been developed during the last decade. Spinel $Li_4Ti_5O_{12}$ (LTO) is known to be a "zero-strain" ion insertion-type anode material for both Li and Mg ions.[4d,e,5] However using a LTO anode for a rechargeable Mg battery also faces the problem of kinetically sluggish Mg insertion/extraction and diffusion in electrode materials. As such Mg insertion behavior into LTO nanoparticles (LTO NPs) is strongly dependent on size.[4d] The activity of LTO NPs drops dramatically with the increase of particle size. Worse, LTO NPs with particle sizes larger than 100 nm are negligible in Mg battery systems. Thus, exploring appropriate approaches for increasing the kinetics of ion insertion-type electrode materials with large particle size, which has more practical advantages, is highly desired in Mg batteries. Considering that the ionic radius of Li^+ is very close to that of Mg^{2+} and the standard reduction potential is lower than that of Mg^{2+}, it could reach higher voltages than the Mg counterpart. If Li^+ is introduced into the Mg system, the whole system could synergistically exploit the advantages of Mg^{2+} and Li^+, which has been validated on a Mo_6S_8 cathode material.[6] In this work, we report a facile approach to eliminate the size dependencies of LTO electrodes during Mg insertion/extraction, resulting in electrode materials with large particle sizes (larger than 100 nm) useful in Mg batteries. Density functional theory calculations reveal possibilities for the thermodynamics of Mg^{2+} and Li^+ co-insertion into large sized LTO electrodes and experimental investigations show that the electrochemical behavior of large sized LTO electrodes combining Mg and Li electrochemistry in Mg battery systems is dependent on the lithium salt concentration in the electrolytes. Tuning the Li^+ activity in the electrolyte properly results in large LTO NPs indicating excellent electrochemical performances in terms of specific capacity, cycling performance, and especially rate performance.

First ab initio calculations are used to examine the thermodynamics underlying the co-insertion of Mg and Li into LTO. In the Li battery, the LTO electrode will turn to $Li_7Ti_5O_{12}$, written as $Li_6[Ti_5Li]^{16d}O_{12}$, for describing the distribution of atoms at fully discharged state. Based on the conclusion of previous work,[4e] $Mg_4[Ti_5Li]^{16d}O_{12}$ is produced in the Mg battery. The microscopic process of Mg/Li co-insertion into LTO indicates two possible mechanisms which are the formation of $[Mg_nLi_{6-1.5n}]^{8a+16c}[Ti_5Li]^{16d}O_{12}$ (solid-solution reaction) or the separation of $[Mg_4]^{8a+16c}[Ti_5Li]^{16d}O_{12}$ and $[Li_6]^{8a+16c}[Ti_5Li]^{16d}$-$O_{12}$ (phase separation reaction), respectively. To study the Li/Mg distribution in the electrode, the formation energy of $[Mg_nLi_{6-1.5n}]^{8a+16c}[Ti_5Li]^{16d}O_{12}$ are calculated, which is defined as Equation (1).

$$\begin{aligned} E_{for} = & E\{[Mg_nLi_{6-1.5n}]^{8a+16c}[Ti_5Li]^{16d}O_{12}\} \\ & - n\,E\{[Mg_4]^{8a+16c}[Ti_5Li]^{16d}O_{12}\}/4 \\ & - (4\text{-}n)E\{[Li_6]^{8a+16c}[Ti_5Li]^{16d}O_{12}\}/4 \end{aligned} \quad (1)$$

[*] N. Wu, H.-R. Yao, Dr. Y.-X. Yin, Prof. Y.-G. Guo
CAS Key Laboratory of Molecular Nanostructure and Nanotechnology
Beijing National Laboratory for Molecular Sciences
Institute of Chemistry, Chinese Academy of Sciences (CAS)
Beijing 100190 (P. R. China)
E-mail: ygguo@iccas.ac.cn
Z.-Z. Yang, Prof. L. Gu
Beijing National Laboratory for Condensed Matter Physics
Institute of Physics, Chinese Academy of Sciences (CAS)
Beijing 100190 (P. R. China)

[**] This work was supported by the National Natural Science Foundation of China (grant numbers 51225204, 21303222, and 21127901), the National Basic Research Program of China (grant numbers 2011CB935700 and 2012CB932900), and the "Strategic Priority Research Program" of the Chinese Academy of Sciences (grant number XDA09010000).

Supporting information for this article, including detailed descriptions of materials synthesis and characterizations including XRD, TEM, STEM, EDS, SEM, and DFT calculations, is available on the WWW under http://dx.doi.org/10.1002/anie.201501005.

The results shown in Figure 1 indicate that the phase separation reaction is energetically favorable. The discussion above is based on the supposition that Mg/Li co-insertion/extraction can occur in LTO. Whether the threshold value of voltage of Li insertion/extraction occurs during the stable electrochemical window of the Mg^{2+} electrolyte is the key of Mg/Li co-insertion/extraction. Such a result is predicted by the calculation of insertion/extraction voltage of Li. For the phase separation property on Mg/Li insertion into LTO, the reaction of Li insertion/extraction can be expressed as $Li_4Ti_5O_{12} + 3\,Li^+ + 1.5\,Mg \leftrightarrow Li_7Ti_5O_{12} + 1.5\,Mg^{2+}$ ($V = -\Delta G/3F$, where ΔG is the change of the free energy between products and reactants and F is the Faraday constant). $G(M^{n+}) \approx nF\varepsilon_{M^{n+}} + E(M)$ (where $\varepsilon_{M^{n+}}$ is the standard reduction potential for M metal). The difference between the Gibbs energy and the total energy is neglected for solid phases. Thus the voltage can be calculated by Equation (2),

$$V = -[E(Li_7Ti_5O_{12}) - E(Li_4Ti_5O_{12}) - 3\,E(Li_{bcc}) + 3F(\varepsilon_{Mg^{2+}} - \varepsilon_{Li^+})]/3F \quad (2)$$

where $E(Li_{bcc})$ is the energy of one Li atom in the body-centered cubic (bcc) metal structure. The calculated voltage of Li insertion/extraction versus Mg^{2+}/Mg is approximately 0.92 V, which occurs during the testing voltage range. The DFT calculation demonstrates that Li/Mg co-insertion/co-extraction into the LTO electrode in the Mg battery system is feasible in theory.

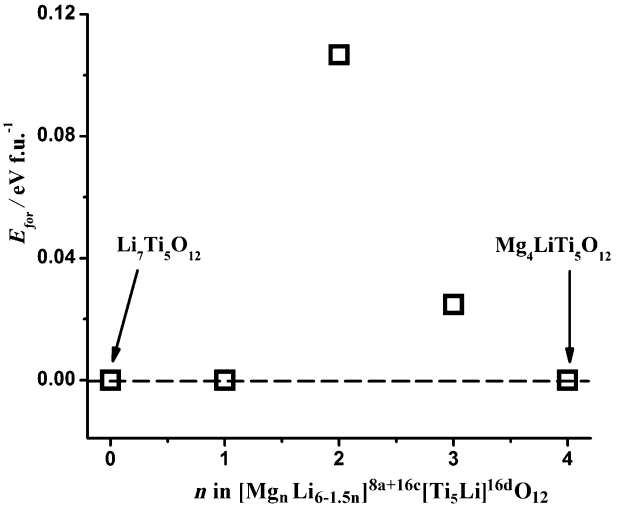

Figure 1. The formation energy of $[Mg_nLi_{6-1.5n}]^{8a+16c}[Ti_5Li]^{16d}O_{12}$ calculated by Equation (1; f.u.$^{-1}$ = per formula unit).

Figure 2a displays the electrochemical performance of the as-prepared LTO (see Figure S1 in the Supporting Information) in Mg batteries with a range of different Li ion-containing $Mg(AlCl_2BuEt_2)_2$/THF 0.25 M electrolytes. The concentration of LiCl in the electrolyte varies from 0 to 0.5 M. The charge–discharge capacity of LTO in the Mg system with pure Mg^{2+} electrolyte is lower than 70 mA h g^{-1} because of the size limitation on the Mg storage performance[4d] in LTO. After tiny amounts of Li^+ are added into the Mg^{2+} electrolyte, the capacity is nearly unchanged. Clearly, the electrochemical property of LTO grows gradually along with the increase in the LiCl concentration. The minimum LiCl concentration for a significant improvement is 0.05 M. Surprisingly, when the Li^+ concentration equals to the optimized concentration (0.25 M), the capacity reaches 175 mA h g^{-1}. Furthermore the LTO/Mg system with Mg^{2+}/Li^+ mixed salt electrolyte shows excellent cycling properties, as demonstrated by a small capacity decay of 0.01 % per cycle over 500 cycles (Figure 2b). Larger LTO particle sizes results in a more notable improvement of Li^+ on the LTO/Mg system (Figures S2 and S3). Notably, LTO NPs with particle sizes larger than 100 nm, which are inactive in the Mg battery with a pure Mg^{2+} electrolyte, show a high capacity of nearly

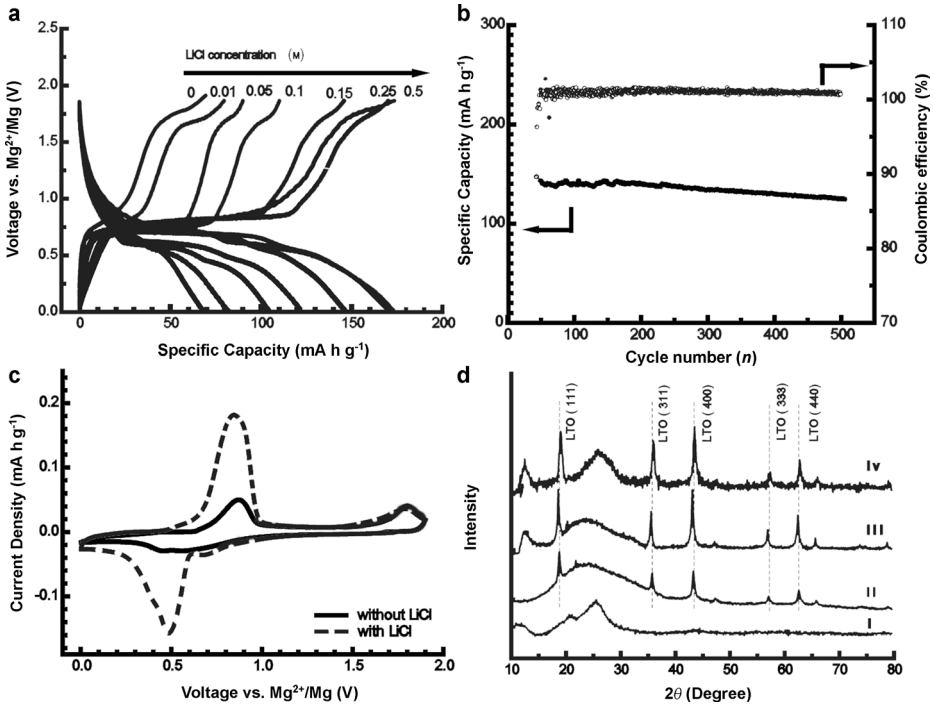

Figure 2. a) Charge–discharge characteristics of the LTO/Mg system with different electrolytes. b) Cycling performance of the cell in 0.25 M LiCl-0.25 M $Mg(AlCl_2BuEt_2)_2$/THF electrolyte cycled under a current density of 60 mA g^{-1}. c) Cyclic voltammograms (CVs) of the cells with different electrolytes for the 11th cycle. d) Ex situ XRD patterns of the LTO electrodes at different charged/discharged states where: i) The mixture of super-P/PVDF was used to prepare the working electrode and a Kapton film was used to cover the electrode. ii) The as-prepared electrode. iii) The electrode at the 20th fully discharged state. iv) The electrode at the 20th fully charged state.

175 mA h g^{-1} in a Mg battery with Mg/Li mixed salt electrolyte (Figure S3). The results indicate that when the Li^+ concentration in Mg^{2+} electrolyte increases to 0.05 M, Li^+ becomes important in improving the performance of large LTO NPs in the Mg system.

To further discuss the effects of Li^+ added into the electrolyte on the reversibility of the LTO electrode, cyclic voltammetry (CV) tests of LTO electrodes with average particle sizes of 15–20 nm were conducted in different electrolytes, which are shown in Figure 2c and Figure S4. With the pure Mg^{2+} electrolyte, all of the characteristic peaks caused by Mg^{2+} inserting into/extracted from the LTO are also well consistent with the previously reported ones[4e] (Figure S4a). The brief reaction mechanism is described in Equations (3)–(5).

$$2\,Li_4Ti_5O_{12} + 4\,Mg^{2+} + 8\,e^- \rightarrow Li_7Ti_5O_{12} + Mg_4LiTi_5O_{12} \quad \text{(discharge process)} \tag{3}$$

$$3\,Li_7Ti_5O_{12} + 5\,Mg_4LiTi_5O_{12} \rightarrow 18\,Li^+ + 18\,e^- + 8\,Mg_{2.5}LiTi_5O_{12} \quad \text{(charge process)} \tag{4}$$

$$Mg_4LiTi_5O_{12} \leftrightarrow Mg_{3.25}LiTi_5O_{12} + 0.75\,Mg^{2+} + 1.5\,e^- \quad (\text{half-deintercalated state, } 0 < x < 2.5)$$
$$\leftrightarrow Mg_{2.5}LiTi_5O_{12} + 1.5\,Mg^{2+} + 3\,e^- \quad (\text{fully deintercalated state, } 0 < x < 2.5) \tag{5}$$

When 0.25 M LiCl is added to the $Mg(AlCl_2BuEt_2)_2$/THF electrolyte, a sharp oxidation peak (Figure S4b) at 0.98 V appears in the 1st CV curve. The result is in good agreement with the calculated voltage of 0.92 V. For the subsequent cycle, the oxidation peak centered at 0.8 V and the reduction peak at 0.5 V grows sharply, whereas the oxidation peak at 1.7 V and the reduction peak at 0.7 V indicate almost no change (Figure S4b). These phenomena are shown more clearly in the comparison of the CV curves for the 11th cycle with the above two kinds of electrolytes (Figure 2c). This implies that in the Mg^{2+}/Li^+ mixed salt electrolyte, the characteristic oxidation/reduction peaks caused by Mg^{2+} have not changed and the dramatic growth peaks at 0.5 and 0.8 V can be attributed to Li^+ inserting in/extracted from LTO with Mg^{2+}, respectively. Different from that with the pure Mg^{2+} electrolyte, the activation process of LTO in Mg^{2+}/Li^+ mixed salt electrolyte becomes inconspicuous because of the contribution of Li^+. The electrochemical reaction occurring in LTO consists of two parts. One is for the Li^+ intercalation/de-intercalation and the other is for the Mg^{2+} insertion/extraction of LTO. The mechanism could be established as shown in Equations (3)–(5) and Equation (6).

$$Li_4Ti_5O_{12} + 3\,Li^+ + 3\,e^- \leftrightarrow Li_7Ti_5O_{12} \tag{6}$$

To confirm the electrochemical reaction occurring in the LTO/Mg system with Mg^{2+}/Li^+ mixed salt electrolyte combining Mg and Li electrochemistry, ex situ X-ray diffractograms of LTO electrodes at different charged/discharged states were recorded (Figure 2d). The results show that the XRD pattern is insensitive to subtle structural changes owing to the "zero-strain" characteristic of LTO during Mg^{2+}/Li^+ insertion/extraction.[4e,5] Recently, the scanning transmission electron microscopy (STEM) technique has been used to investigate the Mg^{2+} and Li^+ insertion/extraction mechanism in LTO and other materials.[4e,7] We also use STEM techniques to further study the Mg^{2+}/Li^+ co-insertion/extraction processes.

Figure 3a and b shows the LTO (Li4) lattice and the corresponding high-angle annular dark field (HAADF) and annular bright field (ABF) STEM images viewed along the [110] direction, respectively. By comparing the repeat unit in Figure 3b with that in Figure 3a, the 32e oxygen sites and 16d titanium sites can be clearly seen in the HAADF image. Considering that Li4 and $Li_7Ti_5O_{12}$ (Li7) have an almost identical $[Ti_5Li]^{16d}O_{12}$ host, they are nearly indistinguishable in the HAADF images without contrast in the Li columns. However, in the ABF images and corresponding line profiles, the Li contrasts can be identified by the 8a (Figure 3b) and 16c sites (Figure 3c) for Li4 and Li7, respectively. In Figure 3d, a significant contrast is observed at the 16c site, meaning that atoms with a large atomic number, Z, emerged at the 16c sites. The corresponding line profile gives a much

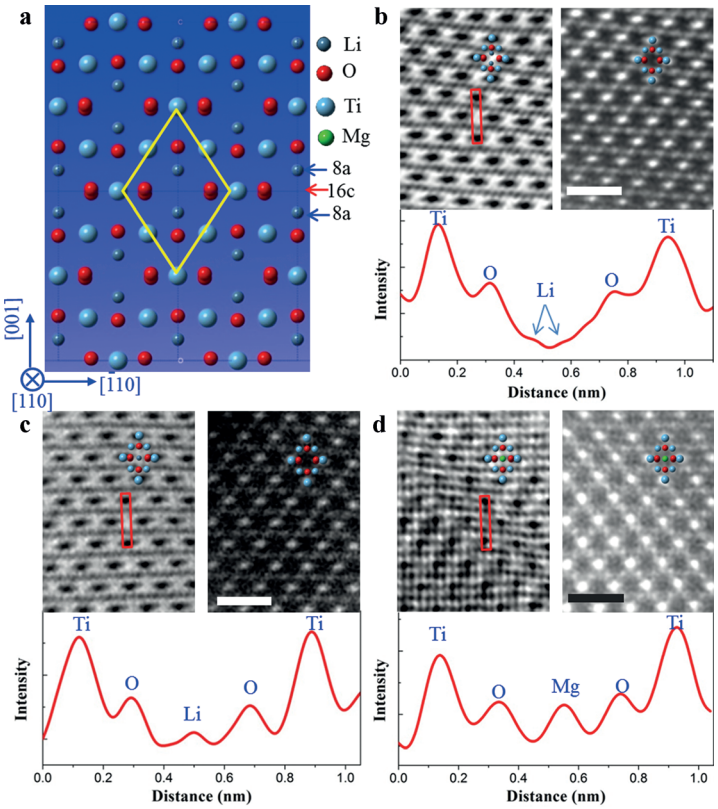

Figure 3. a) Schematic lattice of spinel Li4 viewed from the [110] zone axis, where the Ti, O, and Li columns are highlighted with light blue, red, and dark blue, respectively. b) HAADF, ABF images and ABF line profile for Li4 phase. c) The sample at the fully discharged state with the Li7 phase and d) Mg4Li phase. The Mg column is highlighted with green. Note that the image contrast of the dark dots is inverted and displayed as peaks in the ABF line profile. The scale bar equals 1 nm.

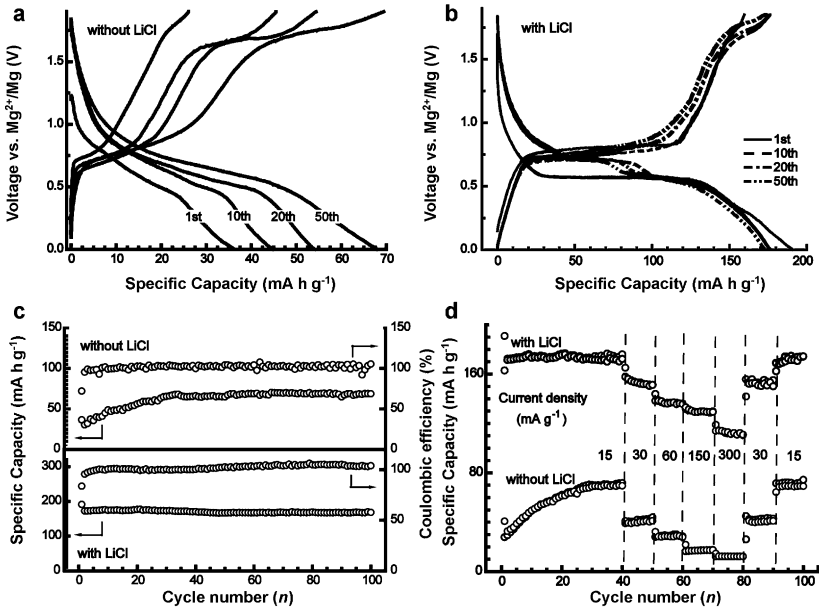

Figure 4. Charge–discharge characteristics of the LTO electrode in rechargeable Mg batteries with different electrolytes under 15 mA g^{-1} (a,b) with pure Mg^{2+} electrolyte (a) and with Mg^{2+}/Li^{+} mixed salt electrolyte (b). c) Comparison of cycling performance of the cells cycled under 15 mA g^{-1}. d) Comparison of the rate capabilities of the LTO electrode in different cells.

clearer picture of the Mg^{2+} position. After the Li4 electrode was discharged to 0 V in the Mg system with Mg^{2+}/Li^{+} mixed ion electrolyte, the Li7 (Figure 3c) and Mg4Li phases[4d] (Figure 3d) are observed at the same time. The direct observation of the two-phase coexistence interface (see Mg4Li/Li7 in Figure S5) agrees well with the completion of the insertion process. These observations confirm that the electrochemical reaction combines Mg and Li electrochemistry in LTO/Mg systems with Mg^{2+}/Li^{+} mixed ion electrolyte.

The charge–discharge capacity of the LTO with pure Mg^{2+} electrolyte for the 1st cycle is only 25 and 35 mA h g^{-1}, respectively (Figure 4a). Even after the activation process, the charge–discharge capacity is still lower than 70 mA h g^{-1}. Surprisingly after addition of 0.25 M LiCl to the electrolyte (Figure 4b), the activity of the Mg^{2+} ions is obviously improved and the LTO sample delivers a discharge capacity of 190 mA h g^{-1} for the 1st cycle, which is 5.5 times that of the sample with pure Mg^{2+} electrolyte. When the cell is stabilized, the reversible capacity is approximately 175 mA h g^{-1}, which is close to the theoretical value of LTO, and the capacity because the contribution of Mg^{2+} intercalation gets to more than 90 mA h g^{-1}. Furthermore the LTO/Mg system with Mg^{2+}/Li^{+} mixed salt electrolyte is highly stable (Figure 4c). After cycling for 167 days, the reversible capacity maintains 175 mA h g^{-1} with a Coulombic efficiency of nearly 100%. Even under a high current density of 300 mA g^{-1}, the specific capacity of LTO in the Mg system with Mg^{2+}/Li^{+} mixed salt electrolyte (Figure 4d) remains at 120 mA h g^{-1}, which is much higher than that with pure Mg^{2+} electrolyte under a low current density of 15 mA g^{-1}. With a similar LTO/Mg system, controlling the Mg^{2+} and Li^{+} insertion chemistry by tuning the Li^{+} activity in the electrolyte leads to a 2.5 times higher charge–discharge capacity at 15 mA g^{-1} and a 12 times higher charge–discharge capacity at 300 mA g^{-1}. These remarkable results inspire us to use this simple method to design a new battery system and develop other new electrode materials, which are inert in the Mg battery.

In conclusion, we have successfully realized the LTO electrode material with a large particle size to be useful in a Mg battery system. By confirming the possibilities of Mg^{2+} and Li^{+} co-insertion into large sized LTO electrodes using density functional theory calculations and experimental investigations, we show the existence of a threshold Li^{+} activity for the large sized LTO electrodes to combine lithiation and magnesiation. By properly tuning the Li^{+} activity in the electrolyte, the large LTO NPs show extraordinary cycle stability, high capacity, and excellent rate capability in rechargeable Mg batteries. Our proposed strategy could be an effective method to improve the electrochemical energy storage capability of other large sized electrode materials in rechargeable Mg batteries.

Keywords: batteries · green chemistry · electrochemical energy storage · electrode materials · nanomaterials

How to cite: *Angew. Chem. Int. Ed.* **2015**, *54*, 5757–5761
Angew. Chem. **2015**, *127*, 5849–5853

[1] a) M. Armand, J.-M. Tarascon, *Nature* **2008**, *451*, 652–657; b) Y.-K. Sun, S.-T. Myung, B.-C. Park, J. Prakash, I. Belharouak, K. Amine, *Nat. Mater.* **2009**, *8*, 320–324; c) Y.-M. Chiang, *Science* **2010**, *330*, 1485–1486; d) J. B. Goodenough, Y. Kim, *Chem. Mater.* **2010**, *22*, 587–603; e) B. Scrosati, J. Garche, *J. Power Sources* **2010**, *195*, 2419–2430; f) J. Chen, F. Cheng, *Acc. Chem. Res.* **2009**, *42*, 713–723; g) L. Hu, H. Wu, F. La Mantia, Y. Yang, Y. Cui, *ACS Nano* **2010**, *4*, 5843–5848; h) Y. Wang, G. Cao, *Adv. Mater.* **2008**, *20*, 2251–2269; i) X. Meng, X. Q. Yang, X. Sun, *Adv. Mater.* **2012**, *24*, 3589–3615; j) T. Zhang, H. Zhou, *Angew. Chem. Int. Ed.* **2012**, *51*, 11062–11067; *Angew. Chem.* **2012**, *124*, 11224–11229; k) Y. Yu, L. Gu, C. Zhu, P. A. van Aken, J. Maier, *J. Am. Chem. Soc.* **2009**, *131*, 15984–15985; l) L. Wang, X. He, J. Li, W. Sun, J. Gao, J. Guo, C. Jiang, *Angew. Chem. Int. Ed.* **2012**, *51*, 9034–9037; *Angew. Chem.* **2012**, *124*, 9168–9171; m) L. Yang, S. Wang, J. Mao, J. Deng, Q. Gao, Y. Tang, O. G. Schmidt, *Adv. Mater.* **2013**, *25*, 1180; n) J.-Y. Luo, W.-J. Cui, P. He, Y.-Y. Xia, *Nat. Chem.* **2010**, *2*, 760; o) J. Jiang, Y. Li, J. Liu, X. Huang, C. Yuan, X. W. Lou, *Adv. Mater.* **2012**, *24*, 5166; p) F. J. Li, H. Kitauraa, H. S. Zhou, *Energy Environ. Sci.* **2013**, *6*, 2302; q) C. Y. Nan, J. Lu, L. H. Li, L. L. Li, Q. Peng, Y. D. Li, *Nano Res.* **2013**, *6*, 469; r) X. Q. Yu, H. L. Pan, W. Wan, C. Ma, J. M. Bai, Q. P. Meng, S. N. Ehrlich, Y. S. Hu, X. Q. Yang, *Nano Lett.* **2013**, *13*, 4721; s) Y.-X. Yin, S. Xin, Y.-G. Guo, L.-J. Wan, *Angew. Chem. Int. Ed.* **2013**, *52*, 13186–13200; *Angew. Chem.* **2013**, *125*, 13426–13441.

[2] a) D. Aurbach, Z. Lu, A. Schechter, Y. Gofer, H. Gizbar, R. Turgeman, Y. Cohen, M. Moshkovich, E. Levi, *Nature* **2000**, *407*, 724; b) P. Novák, R. Imhof, O. Haas, *Electrochim. Acta* **1999**, *45*, 351.

[3] a) N. Amir, Y. Vestfrid, O. Chusid, Y. Gofer, D. Aurbach, *J. Power Sources* **2007**, *174*, 1234; b) D. Aurbach, G. S. Suresh, E. Levi, A. Mitelman, O. Mizrahi, O. Chusid, M. Brunelli, *Adv. Mater.* **2007**, *19*, 4260; c) D. Imamura, M. Miyayama, M. Hibino, T. Kudo, *J. Electrochem. Soc.* **2003**, *150*, A753; d) Z. L. Tao, L. N. Xu, X. L. Gou, J. Chen, H. T. Yuan, *Chem. Commun.* **2004**, 2080; e) Y. Liang, R. J. Feng, S. Q. Yang, H. Ma, J. Liang, J. Chen, *Adv. Mater.* **2011**, *23*, 640.

[4] a) T. S. Arthur, N. Singh, M. Matsui, *Electrochem. Commun.* **2012**, *16*, 103; b) N. Singh, T. S. Arthur, L. Chen, M. Matsui, F. Mizuno, *Chem. Commun.* **2013**, *49*, 149; c) Y. Y. Shao, M. Gu, X. L. Li, Z. Nie, P. J. Zuo, G. S. Li, T. B. Liu, J. Xiao, Y. W. Cheng, C. Wang, J. G. Zhang, J. Liu, *Nano Lett.* **2014**, *14*, 255; d) N. Wu, Y. X. Yin, Y. G. Guo, *Chem. Asian J.* **2014**, *9*, 2099; e) N. Wu, Y. C. Lyu, R. J. Xiao, X. Q. Yu, Y. X. Yin, X. Q. Yang, H. Li, Y. G. Guo, *NPG Asia Mater.* **2014**, *6*, e120, DOI: 10.1038/am.2014.61.

[5] a) Y. Q. Wang, L. Gu, Y. G. Guo, H. Li, X. Q. He, S. Tsukimoto, Y. Ikuhara, L. J. Wan, *J. Am. Chem. Soc.* **2012**, *134*, 7874.

[6] a) N. Pour, Y. Gofer, D. T. Major, D. Aurbach, *J. Am. Chem. Soc.* **2011**, *133*, 6270; b) N. Yoshimoto, S. Yakushiji, M. Ishikawa, *Electrochim. Acta* **2003**, *48*, 2317; c) J. S. Oh, J. M. Ko, D. W. Kim, *Electrochim. Acta* **2004**, *50*, 903; d) Y. Gofer, O. Chusid, H. Gizbar, Y. Viestfrid, H. E. Gottlieb, V. Marks, D. Aurbach, *Electrochem. Solid-State Lett.* **2006**, *9*, A257; e) Y. W. Cheng, Y. Y. Shao, J. G. Zhang, V. L. Sprenkle, J. Liu, G. S. Li, *Chem. Commun.* **2014**, *50*, 9644; f) J.-H. Cho, M. Aykol, S. Kim, J.-H. Ha, C. Wolverton, K. Y. Chung, K.-B. Kim, B.-W. Cho, *J. Am. Chem. Soc.* **2014**, *136*, 16116.

[7] a) S. J. Pennycook, D. E. Jesson, *Phys. Rev. Lett.* **1990**, *64*, 938; b) R. Huang, Y. Ikuhara, *Curr. Opin. Solid State Mater. Sci.* **2012**, *16*, 31; c) M. Kitta, T. Akita, S. Tanaka, M. Kohyama, *J. Power Sources* **2013**, *237*, 26; d) X. Lu, L. Zhao, X. Q. He, R. J. Xiao, L. Gu, Y. S. Hu, H. Li, Z. X. Wang, X. F. Duan, L. Q. Chen, J. Maier, Y. Ikuhara, *Adv. Mater.* **2012**, *24*, 3233.

Received: February 3, 2015
Published online: March 17, 2015

